Development/Plasticity/Repair

Subfunctionalization of a Retinoid-Binding Protein Provides Evidence for Two Parallel Visual Cycles in the Cone-Dominant Zebrafish Retina

Valerie C. Fleisch,[1,2]* **Helia B. Schonthaler,**[2]* **Johannes von Lintig,**[3] **and Stephan C. F. Neuhauss**[1,2]

[1]Institute of Zoology, [2]Swiss Federal Institute of Technology (ETH) Zurich, Department of Biology, and Brain Research Institute, University of Zurich, CH-8057 Zurich, Switzerland, and [3]Department of Pharmacology, Case School of Medicine, Case Western Reserve University, Cleveland, Ohio 44106-4965

In vertebrates, the absorption of a photon results in an 11-*cis* to all-*trans* isomerization of the retinylidene chromophore of cone and rod visual pigments. To sustain vision, metabolic pathways (visual cycles) have evolved that recycle all-*trans*-retinal back to 11-*cis*-retinal. The canonical visual cycle takes place in photoreceptor cells and the adjacent retinal pigment epithelium (RPE). Biochemical analyses provided evidence for the existence of an additional cone-specific visual cycle involving Müller glia cells, but none of its molecular components has yet been identified. Here we took advantage of the zebrafish retina to investigate the role of the cellular retinaldehyde-binding protein CRALBP in this process. We found that the zebrafish genome encodes two *cralbp* paralogs: *cralbp a* and *cralbp b*. These paralogs are differentially expressed in the retina. Cralbp a is exclusively expressed in the RPE, and Cralbp b is localized to Müller cells. We used an antisense morpholino approach to knock down each *cralbp* paralog. Analysis of 11-*cis*-retinal levels revealed that visual chromophore regeneration is diminished under both conditions. Visual performance, as assessed by electroretinography, revealed reduced light sensitivity in both Cralbp a- and Cralbp b-deficient larvae, but it was more pronounced in Cralbp b-deficient larvae. Cralbp b-deficient larvae also exhibited significant deficits in their visual behavior. Together, these data demonstrate that Cralbp expression in Müller cells is essential for cone vision, thereby providing evidence that both the canonical and the alternative visual cycle depend on the same type of retinoid-binding protein.

Key words: retina; zebrafish; photoreceptors; CRALBP/rlbp1; vitamin A; visual cycle

Introduction

In vertebrate photoreceptors, absorbance of light by the visual pigments results in an 11-*cis* to an all-*tran*s isomerization of the visual chromophore (11-*cis*-retinal) and the initiation of the phototransduction signal cascade (Wald, 1968; Stryer, 1986; Schoenlein et al., 1991; McBee et al., 2001; Palczewski et al., 2006). To sustain vision, 11-*cis*-retinal must be recycled in a complex sequence of enzymatic reactions, collectively named the visual cycle. The canonical visual cycle takes place in two separate compartments of the retina. In the photoreceptor outer segments, all-*trans*-retinal is converted to all-*trans*-retinol. Subsequently, all-*trans*-retinol is transported to the second compartment, the retinal pigment epithelium (RPE) and esterified into retinyl es-

ters (REs). REs are then converted to 11-*cis*-retinol by the action of a retinoid isomerase encoded by the *Rpe65* gene (Jin et al., 2005; Moiseyev et al., 2005; Redmond et al., 2005). Finally, 11-*cis*-retinol is oxidized to 11-*cis*-retinal and shuttled back to the photoreceptor outer segment. The reactions in the RPE depend on cellular retinaldehyde-binding protein (CRALBP), which acts as a substrate carrier to chaperone retinaldehyde through an aqueous milieu (Winston and Rando, 1998; Stecher et al., 1999). Mice with an inactivated *Cralbp* gene exhibit impaired visual pigment regeneration. Both 11-*cis*-retinal production and dark adaptation after illumination are delayed and coincide with an accumulation of all-*trans*-retinyl esters, consistent with a role in the canonical visual cycle (Saari et al., 2001).

The expression of CRALBP in Müller glia cells of the inner retina suggests an additional function of this protein (Bunt-Milam and Saari, 1983; Saari and Bredberg, 1987). One possibility might be that CRALBP expressed in Müller glia cells participates in cone visual pigment regeneration. Recent biochemical studies with cone-dominated retinas isolated from chicken and ground squirrel provided evidence for such an alternative visual cycle for cones (Mata et al., 2002, 2005; Muniz et al., 2007). These biochemical data are supported by *in vivo* studies in zebrafish (*Danio rerio*) larvae, showing that the loss of Rpe65, the retinoid isomerase of the canonical visual cycle, only marginally affects cone vision (Schonthaler et al., 2007).

Thus far, none of the molecular components of this putative alternative visual cycle has been molecularly identified. In the present study, we show that the genome of zebrafish encodes two paralogs of *cralbp* (*cralbp a* and *b*), which show spatially nonoverlapping expression: *cralbp a* is expressed in the RPE and *cralb b* is expressed in Müller glia cells. This unique genetic constellation allows the analysis of the function of Cralbp either in the RPE or Müller cells. To approach this, we used an antisense morpholino approach to knock down either one or both proteins. In respective Cralbp a- and Cralbp b-deficient larvae, we functionally tested visual performance by electroretinography (ERG) and visual behavior analysis and additionally performed HPLC profiling for 11-*cis*-retinal. Together, our data demonstrate that Cralbp expression in both Müller cells and the RPE is required for cone visual pigment regeneration.

Materials and Methods

Fish care and strains. Zebrafish of the Tü strain were used as the wild-type strain (Dahm et al., 2005). Zebrafish were maintained at 28°C under a 14/10 h light/dark cycle and bred and crossed as described previously (Westerfield, 1994). Larvae were raised in E3 medium [containing (in mM) 5 NaCl, 0.17 KCl, 0.33 CaCl$_2$, and 0.33 MgSO$_4$] until 5 d postfertilization (dpf).

Cloning. Putative zebrafish *cralbp* genes were identified via a homology search of the Zv7 Ensembl database (http://www.ensembl.org/Danio_rerio) using the human CRALBP protein sequence as query. Total RNA was isolated from 5 dpf zebrafish larvae using the RNAeasy kit (QIAGEN) according to the manufacturer's instructions. cDNA was synthesized using the SuperScript III Reverse Transcriptase Kit (Invitrogen) as described in the manual. To amplify the coding sequence from the cDNA, the following primers were used. cralbp a: sense, AACGTTGCATTGAG-TATTTGAAGC; antisense, GAGACTTATCCAGTTTCGCTTGG. cralbp b: sense, TGGAATAGTTGACGGTTCATTCC; antisense, AAAAGGGCTGTGTCTTCAGATC.

To obtain 5′ and 3′ sequences of the *cralbp* cDNA, RACE-PCR was performed with the SMART RACE cDNA Amplification Kit (Clontech). PCR products were cloned into the pCRII-Vector (Clontech) and sequenced with T7 and SP6 primers (GenBank accession number for *cralbp a*, EU348854, and for *cralbp b*, EU348853).

In situ *hybridization (whole mount and slides).* Sense and antisense probes for *in situ* hybridization (ISH) were transcribed *in vitro* from a linearized pCRII-Vector containing the full-length *cralbp a* and *b* coding sequence using SP6 and T7 polymerases, respectively, in the presence of digoxigenin-coupled nucleotides (DIG RNA Labeling Kit; Roche Molecular Biochemicals). Transcripts were hydrolyzed to obtain fragments of ~300–500 nt length. To prevent melanization of skin melanocytes and the RPE, embryos used for ISH were treated with 0.2 mM 1-phenyl-2-thiourea (PTU; Sigma). PTU-treated embryos were staged, fixed in 4% paraformaldehyde (PFA) in 1× PBS, pH 7.3, at 4°C overnight, dehydrated in a standard methanol series, and stored in 100% methanol at −20°C. ISH was performed using an automated ISH apparatus (Hölle &
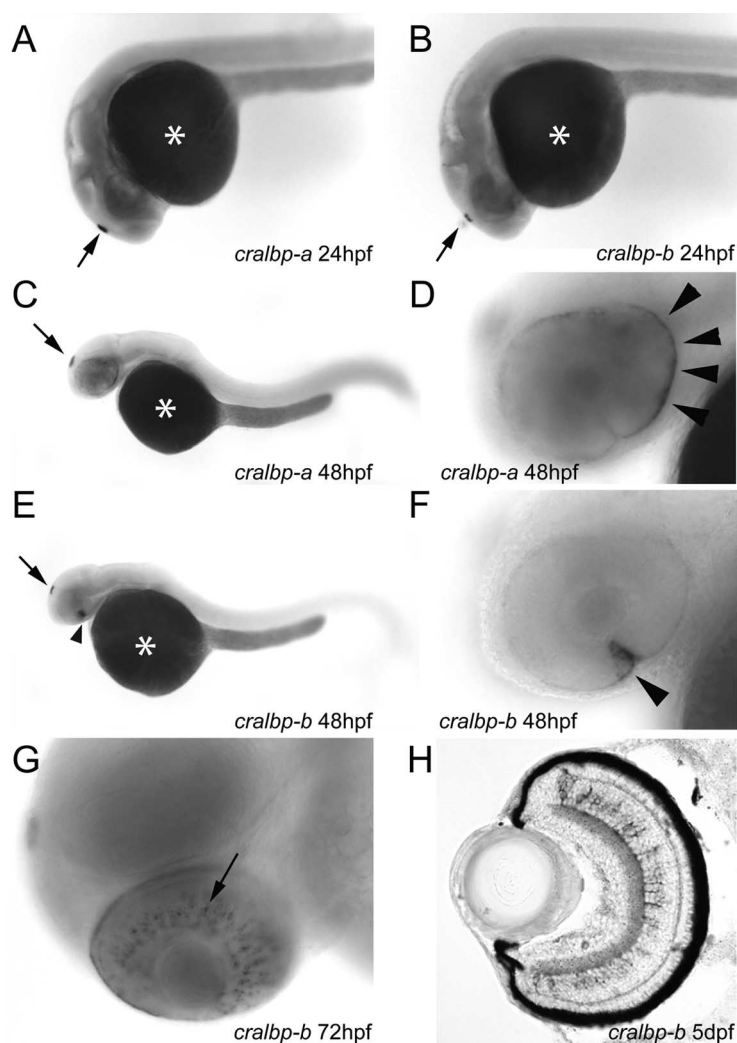

Figure 1. Spatiotemporal expression analysis of *cralbp a* and *b* paralogs during zebrafish development. *A*, *B*, *cralbp a* and *b* mRNA expression is first detected at 24 hpf in the pineal gland (arrows). *C–F*, At 48 hpf, *cralbp a* starts to be expressed in the RPE (arrowheads in *D*), whereas *cralbp b* is detected in the choroid fissure (arrowheads in *E*, *F*). *G*, *H*, Subsequently, the expression of *cralbp a* becomes more intense in the cells of the RPE, whereas *cralbp b* expression appears specifically in Müller glia cells. Arrows in *A–C* and *E* point to the pineal gland, arrowheads in *D* point to the RPE, and arrowheads in *E* and *F* point to the choroid fissure. Asterisks mark the larval yolk.

Hüttner). Hybridization with probes was performed overnight at 62°C. Detection was performed with an alkaline phosphatase-coupled anti-digoxigenin Fab fragment (Roche) and NBT/BCIP (nitroblue tetrazolium/5-bromo-4-chloro-indolyl phosphate) staining buffer. Stained embryos were cleared with 50% methanol/50% glycerol and transferred into 100% glycerol for imaging.

Standard histology. Larvae (5 dpf) were fixed for 1 h in 4% PFA in 1× PBS (0.8% NaCl, 0.02% KCl, 0.02 M PO$_4$, pH 7.3). After two washing steps with 1× PBS, they were dehydrated through a series of dehydration steps ranging from 50% to 100% ethanol. For preinfiltration, larvae were incubated 1:1 in 100% ethanol and Solution A [25 ml of Technovit 7100 (Heraeus Kulzer) plus 0.25 g of Hardener 1] two times for 30 min each. For infiltration, larvae were incubated in 100% Solution A at 4°C overnight. For polymerization, Solution A was mixed with Hardener II (15:1), and finally, larvae were embedded in the polymerization solution.

Sections (3–5 μm) were cut using a rotation microtome. Slides were dried, stained with Richardson (Bromeis) solution (1% methylene blue, 1% Borax, 1% azur II, in a ratio of 1:1:2), and covered in Entellan (Merck).

Immunostaining. Wild-type and morpholino-injected larvae were raised in E3 medium containing 0.2 mM PTU to prevent development of pigment in the RPE.
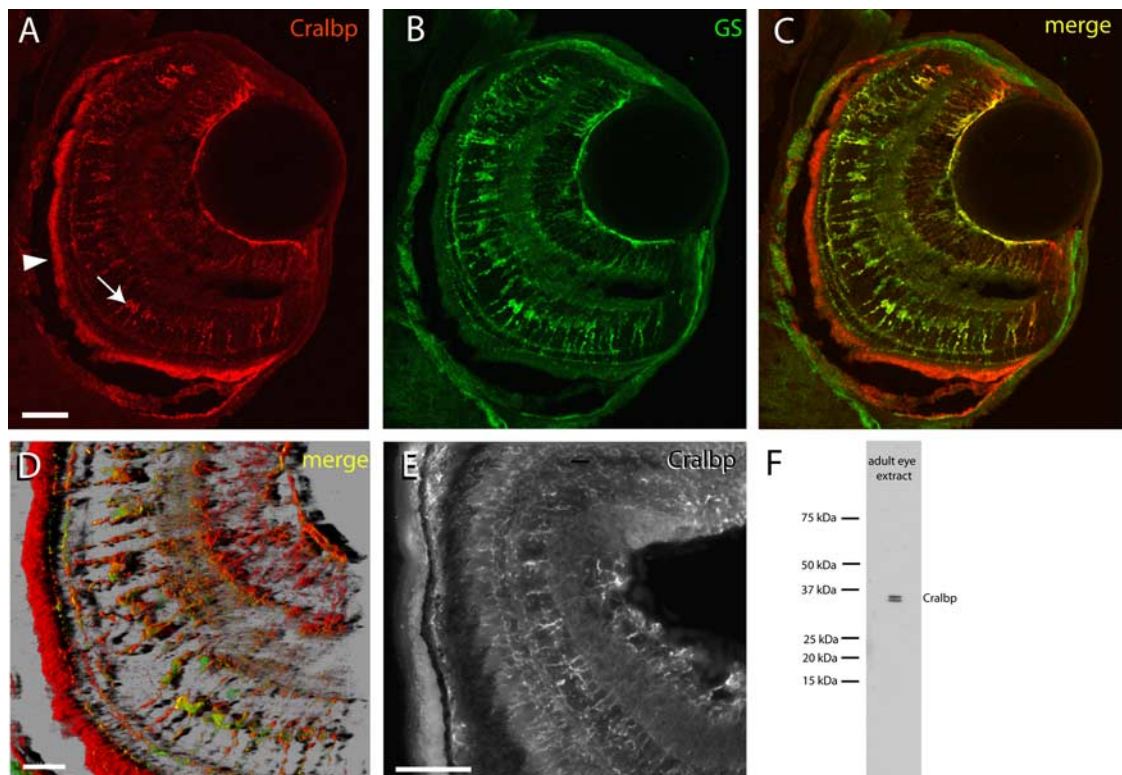
Figure 2. CRALBP antiserum detects both zebrafish Cralbp proteins on immunostaining. **A**, Control (5 dpf; wild-type) larval sections; the arrowhead points to RPE, and the arrow points to Müller glia cell bodies. **B–D**, Colocalization of Cralbp staining with glutamine synthetase staining. **B**, Immunostaining for glutamine synthetase in radial section of 5 dpf wild-type larvae. **C**, Merge picture of **A** and **B**. **D**, Higher magnification of double staining using the CRALBP and GS antisera. **E**, Immunostaining of adult section using the CRALBP antiserum. The arrowhead points to RPE, and the arrow points to Müller glia cell bodies. Scale bar: **A**, **E**, 30 μm; **D**, 15 μm. **F**, Western blot performed on protein extract of adult zebrafish eyes, incubated with the Cralbp antiserum (generously provided by J. Saari).

For immunohistochemistry, larvae were fixed for 45 min in 4% paraformaldehyde in 1× PBS, washed with 1× PBS, and incubated overnight in 30% sucrose at 4°C. Fixed larvae were embedded in Tissue Tec medium (Sakura Finetek Europe) and immediately frozen in liquid nitrogen. Sections of 16 μm were cut using a cryotome, dried for 30 min at room temperature, and stored at −80°C.

Before using the slides for immunostaining, they were dried for 1 h at 37°C, washed in 1× PBS, and incubated for 4 h with blocking solution (10% normal goat serum, 1% bovine serum albumin in 1× PBS containing 0.3% Tween). Subsequently, sections were incubated with the primary antibody at 4°C overnight, washed two times with 1× PBS, and incubated with the secondary antibody for 1–2 h at room temperature. Finally, slides were washed two times with 1× PBS, covered with Kaisers Glyceringelatin (Merck), and stored at −20°C.

For Cralbp immunostaining, CRALBP antiserum (kindly provided by Dr. Johnathan Saari, University of Washington, Seattle, WA) was used at a 1:500 dilution. For double staining with glutamine synthetase (GS), the anti-GS antibody (Millipore Bioscience Research Reagents) was used in a 1:1000 dilution. For immunostaining for rods, the 1D1 antibody (kindly provided by Ann Morris, Florida State University, Tallahassee, FL) was used 1:100, and staining for cones was performed by using the Zpr1 antibody (Zebrafish International Resource Center) in a 1:20 dilution. Alexa Fluor 488 and Alexa Fluor 568 (Invitrogen) directed against rabbit (for Cralbp) or mouse (for all of the other antibodies) were used as secondary antibodies.

Antisense morpholino knock-down. Specific morpholino nucleotides directed against zebrafish *cralbp a* (GAAATGTTCCACTAACAACCGC-CAT) and *cralbp b* (GCCATAGTGCTCAGATTCTCCACGG) as well as a control were ordered from Gene Tools. Morpholinos were diluted in 1× Danieau's solution [58 mM NaCl, 0.7 mM KCl, 0.4 mM MgSO$_4$, 0.6 mM Ca(NO$_3$), 5 mM HEPES] containing 0.2% phenol red (for color indication purposes) to the desired concentration. Diluted morpholinos were injected into the 1–2 cell-stage embryo.

Quantification of mRNA levels by real-time PCR. Total RNA from morpholino-injected larvae was isolated using TRIzol (Invitrogen). The isolated RNA was used to generate cDNA by using Ready-To-Go You-Prime First-Strand Beads (GE Healthcare), following the manufacturer's protocol. For the real-time PCR (RT-PCR) analysis, two different primer pairs spanning an exon boundary for each *cralbp a* and *b* gene were designed: *cralbp a*, sense: TGAGCTTGCTAAAGGTGTTCAGG and GTCAAACCCCTGATGAAGAGC; antisense: TCAGGATAATCCC-GTCTGAAGC and GTGATCTTGCCGTCATATTTGG. *cralbp b*, sense: TTGAACATCTGACTGTGAAAGACC and CTGCCGTGCCTACTGTG-TAATCC; antisense: GCCTGCCTTGTCTTTAATCATGG and ATCA-CATGCACAGCCTTAAACC. *gapdh* (glyceraldehyde-3-phosphate dehydrogenase), sense: CACAACCAAATCAGGCATAATGG; antisense: CATGTAATCAAGGTCAATGAATGG.

Real-time PCR was performed with SYBR Green on an Opticon 2 monitor fluorescence thermocycler (MJ Research). Loading was normalized to *gapdh* expression, and results were normalized to control larvae.

Photography. Immunostaining and histological sections were photographed under an Olympus BX61 microscope, and pictures were taken with the F-View camera (Olympus). Images were edited using the Olympus Cell Soft Imaging Software.

Pictures of the *cralbp a* and *b* expression analysis were taken using an Axioscope 2Mot (Zeiss) connected to an AxioCamHR color camera using the AxioVision 3.0 software (Zeiss).

Optokinetic response measurements. Larval OKR responses were measured as described previously (Rinner et al., 2005a). Single larvae were placed upright in the center of a 35 mm Petri dish containing 3% prewarmed (28°C) methylcellulose for immobilization. Moving square gratings of different contrasts were projected onto a screen by a Proxima 4200 DLP projector. Eye movements triggered by the visual stimulation were recorded by means of an infrared-sensitive CCD camera. Custom-developed software on the basis of LabView IMAQ (National Instru-
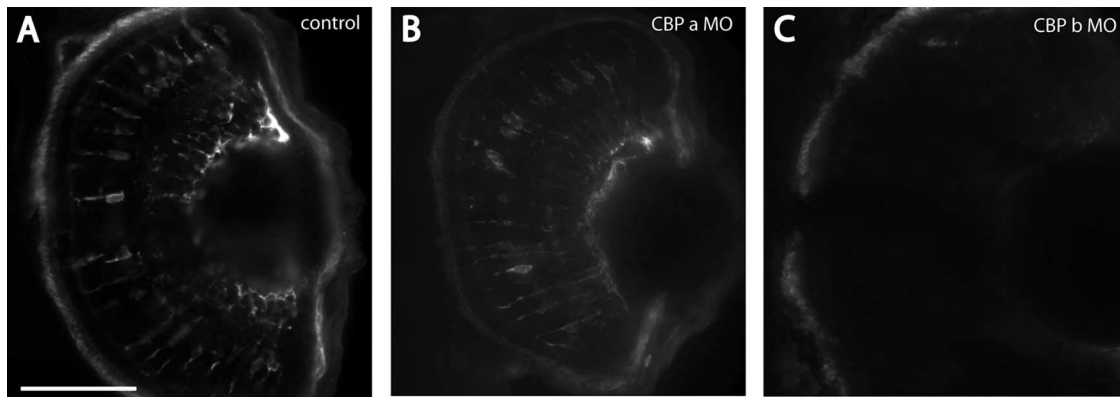
Figure 3. Injection of morpholino oligonucleotides results in reduction of Cralbp a and b protein levels. *A*, Immunostaining using the CRALBP antiserum on 5 dpf control (wild-type) larval section. *B*, Immunostaining of section taken from 5 dpf *cralbp a* morpholino-injected (1 mM) larva. *C*, Immunostaining of 5 dpf *cralbp b* morpholino-injected (700 μM) larva. Scale bar, 50 μm.

Table 1. Relative expression levels of *cralbp a* and *b* in *cralbp a* (MO*a*), *b* (MO*b*), and double (MO*a/b*) morpholino-injected larvae normalized to controls

RNA samples	Relative expression of *cralbp a* to controls	Relative expression of *cralbp b* to controls
MO*a*	0.22 (±0.17)	1.51 (±3.59)
MO*b*	0.71 (±1.02)	0.29 (±0.21)
MO*a/b*	0.29 (±0.15)	0.28 (±0.23)

Data are shown as means; SD is depicted in parentheses.

ments, version 5.1) was used to control stimulation and camera, and to analyze the resulting images.

Statistical analysis was performed using a bootstrap resampling test of pooled data. A detailed description of this statistical method is provided (Rinner et al., 2005b). The significance level has been chosen as 5% for all measurements.

ERG recordings. Recordings were done as described previously (Makhankov et al., 2004). Larvae (5 dpf) were dark-adapted for at least 30 min before starting the measurements. Larvae were anaesthesized with a drop of 0.5% 3-aminobenzic acid ethyl ester, in H_2O, pH 7 and positioned right above the reference electrode. The recording electrode was positioned onto the cornea, without damaging the eye. A light stimulus of 100 ms duration and light intensity of 6000 lux was used to elicit a saturating response. Varying light intensities of 5 log units (log −4 to log 0; log 0 corresponding to 6300 lux) were used for measuring the intensity–response function. The response of each single larva was measured five times and then averaged. Statistical analysis was done using GraphPad Prism 4 (GraphPad Software) and graphs were drawn using Origin version 7 (OriginLab).

Retinoid analysis. Zebrafish larvae (4 dpf) were dark-adapted overnight. Before illumination, 5 dpf larvae were placed into Petri dishes under dim red light. The bottom and the sides of these dishes were coated with light-reflecting aluminum foil. The larvae were then illuminated for 20 min with 10,000 lux using a KL 1500-T electronic fiber optic device (Schott). On illumination, larvae were dark-readapted for 45 min, then immediately collected under dim red light, killed on ice, and stored at −70°C. Retinoids were extracted under monochromatic light (695 nm) and subjected to HPLC separation as described previously (Schonthaler et al., 2007). For quantification of the molar amounts of retinoids, peak integrals were scaled with defined amounts of reference substances and were quantified using 32 Karat software (Beckman Instruments) as described previously (von Lintig and Vogt, 2000).

Results
The zebrafish genome harbors two *cralbp* orthologs
The cone-dominant retina of the zebrafish is ideally suited for the genetic analysis of photoreceptor function (Rinner et al., 2005a; Schonthaler et al., 2007). We used a combination of bioinformatics and cDNA cloning strategies to isolate genes coding for *cralbp*.

We identified two paralogs of mammalian *Cralbp* and denoted them as *cralbp a* and *cralb b*. By BLAST (basic local alignment search tool) analysis and sequence alignments using the Zv7 assembly of the zebrafish genome (http://www.ensembl.org/Danio_rerio/index.html), the two cloned genes were located to two different chromosomes, *cralbp a* to chromosome 25 and *cralbp b* to chromosome 7. Both share a high degree of identity to the mouse and human orthologs at the level of the deduced amino acid sequences. Phylogenetic analysis (ClustalW, MegAlign; DNAStar) confirmed that these paralogs are true orthologs to the mammalian *Cralbp* gene (supplemental Fig. 3, available at www.jneurosci.org as supplemental material).

In linear alignments, these two paralogs share an identity of ~76% at the nucleic acid and 80% at the amino acid level (supplemental Figs. 1–3, available at www.jneurosci.org as supplemental material).

Zebrafish *cralbp* paralogs show complementary retinal expression
To determine the developmental expression of these genes, we performed whole-mount *in situ* hybridization experiments with embryos and larvae of different developmental stages. Both *cralbp a* and *cralbp b* mRNA expression first became detectable in the pineal gland at 24 h postfertilization (hpf) (Fig. 1*A,B*). The pineal is a photosensitive organ in the dorsal diencephalon. Expression in the pineal gland of both *cralbp* paralogs persisted when development proceeded and was maintained into adulthood.

At 48 hpf, the expression of the two *cralbp* paralogs also became detectable in the retina but was strikingly complementary. *Cralbp a* was expressed in the developing RPE and *cralbp b* was expressed in the choroid fissure (Fig. 1*C–F*). At later developmental stages, the expression of *cralbp a* spread out through the RPE (Fig. 1*C,D*) and *cralbp b* was specifically detected in Müller glia cells of the inner retina (Fig. 1*G,H*). This expression pattern was preserved in all developmental stages examined and suggests a subfunctionalization of the two Cralbp proteins to different compartments in the zebrafish retina.

To confirm these results on the protein level, we used an antibody raised against mammalian CRALBP (generously provided by J. Saari), which detected two bands corresponding to the two zebrafish Cralbp proteins on a Western blot (Fig. 2*F*), and labeled Müller glia cells and RPE cells in the zebrafish retina just as in the mouse retina (Fig. 2*A,C–E*). This staining pattern was consistent with mRNA expression (see above), suggesting that the antibody
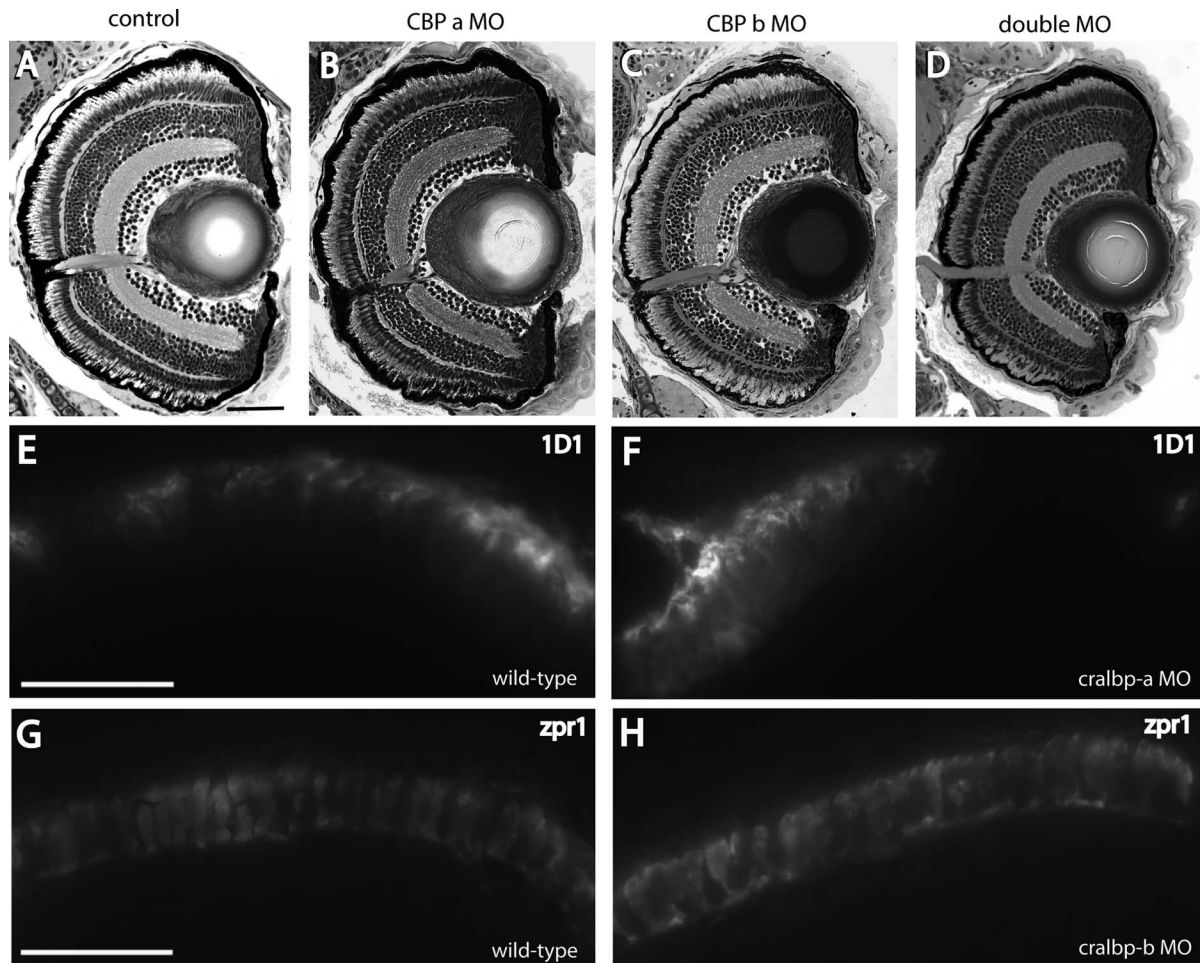
control CBP a MO CBP b MO double MO

Figure 4. Assessment of retinal and photoreceptor integrity in *cralbp a*, *b*, and double-morpholino-injected larvae. **A–D**, Radial sections of 5 dpf control and morpholino-injected larvae, stained with Richardson (Bromeis) solution. **A**, Control (wild-type); **B**, *cralbp a* morpholino-injected larva (1 mM); **C**, *cralbp b* morpholino-injected larva (700 μM); **D**, coinjected larva (*cralbp a*, 800 μM; *cralbp b*, 500 μM). **E–H**, Immunostaining for rod and cone outer segments using 1D1 (rod-specific) (**E**, **F**) and zpr1 (cone-specific) (**G**, **H**) antibodies. **E**, Wild-type retina stained with 1D1; **F**, retina of *cralbp a* morpholino-injected larva (1 mM) stained with 1D1; **G**, wild-type retina stained with zpr1; **H**, retina of *cralbp b* morpholino-injected larva (700 μM) stained with zpr1. Scale bars, 50 μm.

specifically recognizes both *cralbp* paralogs in the larval and the adult zebrafish retina.

To confirm that the cells labeled in the inner retina were Müller glia cells, we performed double labeling experiments with the Müller glia cell-specific marker glutamine synthetase (anti-GS). Indeed, we found that Cralbp b and GS are colocalized, thus demonstrating that the Cralbp b protein is expressed in Müller glia cells (Fig. 2B–D).

Generation of Cralbp deficient larvae

The complementary expression patterns of the two *cralbp* genes allowed us to study the function of the two paralogs separately by loss-of-function studies. Toward this end, we designed antisense morpholino nucleotides (MOs) targeted against the translational start sites of either *cralbp a* or *cralbp b*. This approach is routinely used to specifically knock down gene functions in different embryonic compartments (Nasevicius and Ekker, 2000; Rinner et al., 2005a; Schonthaler et al., 2007). Injection of both *cralbp* MOs did not cause any developmental malformations. Injected larvae are indistinguishable from mock or control injected larvae throughout development.

Immunohistological staining with the CRALBP antiserum showed that expression of the proteins was highly diminished or absent in the larval retina at 5 dpf . Injection of the MO targeted

against *cralbp a* (*cralbp aMO*) highly diminished labeling for Cralbp in the RPE but did not affected Cralbp protein levels in Müller glia cells (Fig. 3B). In contrast, injection of morpholino targeting *cralbp b* (*cralbp bMO*) led to a highly reduced staining for Cralbp in the inner retina but did not affect staining for Cralbp in the RPE (Fig. 3C).

The CRALBP antiserum recognizes two bands of the predicted molecular weight for both Cralbp proteins on a Western blot (Fig. 2F). Unfortunately, in Western blot analysis, Cralbp protein levels were below the detection limit in protein extracts of 5 dpf larvae. Hence, we decided to take an alternative approach using quantitative real-time PCR analysis on reverse-transcribed cDNA to get an indirect estimation of the remaining Cralbp protein levels in larvae that had been injected with morpholinos against *cralbp a*, *b*, or both.

We observed a reduction of ~78% of *cralbp a* mRNA in *cralbp a* morpholino-injected larvae and ~70% in double-morpholino-injected larvae. Similarly, a reduction of ~70% of *cralbp b* mRNA in *cralbp b* and double-injected larvae was detected (Table 1). Interestingly, we also saw an increase of *cralbp b* mRNA in *cralbp a* morpholino-injected larvae and vice versa, which was highly variable and might be caused by a compensatory mechanism (Table 1).

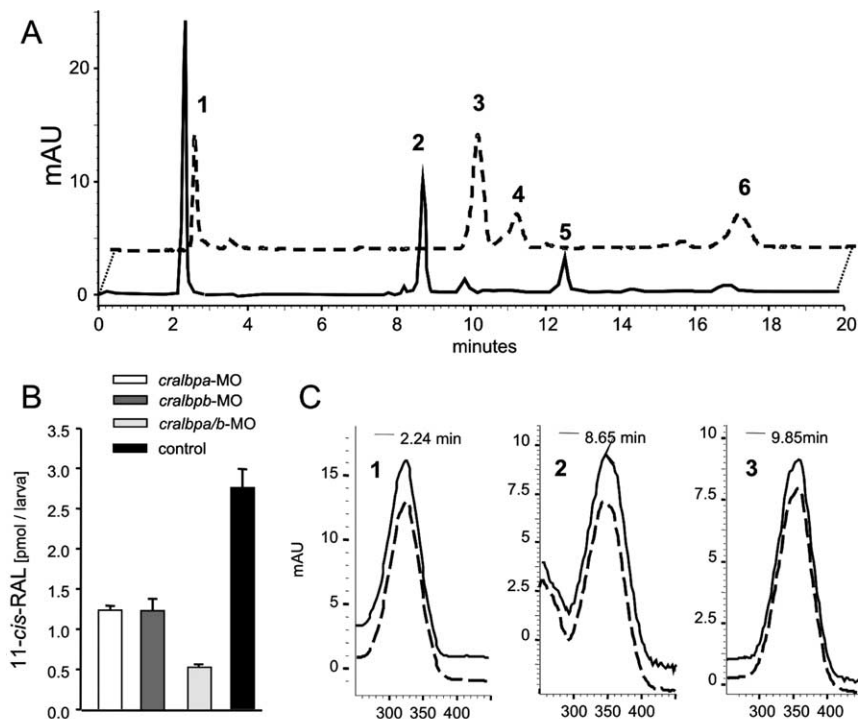Hence, we can manipulate protein expression of the two

Figure 5. Levels of 11-*cis*-retinal in 5 dpf larvae. **A**, HPLC traces at 325 nm of lipophilic extracts isolated from dark-adapted 5 dpf larval eyes (solid line) and the remaining trunks including the yolk (dashed line). **B**, 11-*cis*-Retinal levels in *cralbp a*, *cralbp b*, and co-morpholino-injected larvae compared with control larvae. All larvae were bleached (10,000 lux) and dark-readapted for 45 min before analysis. The values give the mean ± SD of three independent experiments. **C**, Spectral characteristics of different vitamin A derivatives (solid line) compared with authentic standard substances (dashed line). 1, retinyl esters; 2, 11-*cis*-retinal-oxime (syn); 3, all-*trans*-retinal-oxime; 4, 13-*cis*-retinal-oxime (syn and anti), 5, 11-*cis*-retinal-oxime (anti); all-*trans*-retinal (anti).

cralbp paralogs in a cell-specific manner either in the inner retina (Cralbp b) or in the RPE (Cralbp a).

To examine the effect of reduced Cralbp levels on the integrity of the retina, standard histological sections of 5 dpf control and morpholino-injected larvae were analyzed for retinal morphology and layering. No morphological alterations were detected in *cralbp a*, *b*, and double-morpholino-injected larvae, and no cell loss was visible (Fig. 4A–D). To look more closely at photoreceptor morphology, we performed immunostaining for red-green double cones using the Zpr1 (Fret43) antibody and for rods using the 1D1 antibody. Cone and rod outer segments appeared normal in all morpholino-injected larvae (Fig. 4E–H).

cralbp morpholino-injected larvae have reduced levels of 11-*cis*-retinal

To assess the effect of the targeted knock-down of different *cralbp* paralogs on ocular retinoid metabolism, we determined 11-*cis*-retinal levels. For this purpose, 4 dpf morpholino-injected larvae and control siblings (50 larvae per group) were raised under a standard day-and-night light regimen (14/10 h). The larvae were dark-adapted overnight before analysis. At 5 dpf, larvae were bleached by bright light (10,000 lux) for 20 min and were dark-readapted for 45 min. We then determined 11-*cis*-retinal levels in whole larvae as a measure for the visual pigment content in the eyes. In a control experiment, we showed that 11-*cis*-retinal is only present in the eyes and absent in other body parts of the larva including the yolk (Fig. 5A). Importantly, 11-*cis*-retinal can be distinguished by its retention time and spectral characteristics from the all-*trans*- and 13-*cis*-retinal stereoisomers, which are abundant in the larval yolk (Fig. 5A,C). In repeated experiments

(*n* = 3), we found that the amounts of 11-*cis*-retinal were reduced in both *cralbp a* and *b* morpholino-injected larvae. Knocking-down either of the Cralbp proteins reduced the amounts of 11-*cis*-retinal to ~50% of wild-type control levels (Fig. 5B), and coinjection of both morpholinos resulted in a further reduction of 11-*cis*-retinal levels down to ~25% of control levels (Fig. 5B). Interestingly, a comparable reduction of the 11-*cis*-retinal levels was reported in Rpe65-deficient zebrafish larvae devoid of visual pigment regeneration via the canonical visual cycle. Thus, we concluded that both Cralbp a in the RPE and Cralbp b in Müller cells are required for 11-*cis*-retinal regeneration in zebrafish.

Cralbp-deficient larvae have diminished visual performance

The electroretinogram records the sum field electrical potential of the eye and is a sensitive physiological tool to assess outer retina function in larval zebrafish.

We used a 100 ms light stimulus (of 5 log units of light intensities with the highest light intensity/log 0 corresponding to 6300 lux) to elicit an ERG response in 5 dpf control and morpholino-injected larvae on dark adaption. Typical traces are depicted in Figure 6A, and B shows a graph representing the intensity response functions. Morpholino-injected larvae showed decreased b-wave amplitudes at all light intensities compared with controls. Moreover, the intensity response function was shifted along the intensity axis (Fig. 6A,B). For a quantification of responses, we used the b-wave amplitude, which is a robust measure for outer retinal function (Rinner et al., 2005b). A quantification of saturated responses (to a light stimulus of 6000 lux) is depicted in Figure 6C. Under this condition, the b-wave amplitude of *cralbp a* morpholino-injected larvae was decreased to 128.8 μV compared with control larvae with a b-wave amplitude of 273.9 μV. In *cralbp b* morpholino-injected larvae, the b-wave amplitude showed an even stronger decrease to 77.02 μV, and combined injections of both MOs resulted in a reduction of the b-wave amplitude to 57.5 μV. We induced a MO concentration-dependent decrease of the b-wave amplitude in *cralbp b* morpholino-injected larvae, demonstrating the specificity of the measured effects in ERG analysis (data not shown).

Together, these data demonstrate that the deficiency of either Cralbp reduced light responsiveness of the larval retina. Importantly, Cralbp b deficiency of Müller cells had a more pronounced effect than Cralbp a deficiency of the RPE, indicating that it is more relevant for visual pigment regeneration in cones.

Visual behavior is affected in Cralbp b-deficient larvae

To directly assess the effects of Cralbp deficiency on visual performance, we used a vision-dependent optokinetic response test. Tracking eye movements were triggered by movement in the visual field. To compare visual performance between *cralbp* morpholino-injected larvae and control larvae, we measured a contrast sensitivity function. Visual performance was not af-

fected in *cralbp a* morpholino-injected larvae (Fig. 7A). In contrast to that, *cralbp b* morpholino-injected larvae showed a significantly ($p < 0.05$) decreased visual performance at higher contrast gratings (Fig. 7B). Thus, larvae suffering from Cralbp deficiency of Müller cells show an impaired visual behavior under light conditions when cones are functional.

Discussion

The photoisomerization of the chromophore 11-*cis*-retinal to all-*trans*-retinal in the photoreceptor outer segments is the first step in phototransduction. Continuous vision necessitates the regeneration of the visual chromophore in a process termed the visual cycle. The canonical visual cycle is well described for visual pigment stemming from rod photoreceptors. It is located in both photoreceptor cells and the RPE.

Recently, evidence has accumulated that in cone-dominant species another visual cycle exists that is mainly concerned with regeneration of visual pigment from cone photoreceptors. The competition for 11-*cis*-retinal, the visual chromophore for both rod and cone photoreceptors, might have required the evolution of rod- and cone-specific regeneration mechanisms. Both photoreceptor types work at different light intensities, so that the high demand of visual pigment for rods at photopic conditions might restrict the availability of the visual chromophore for cones in their working range (Mata et al., 2002; Muniz et al., 2007).

The existence of such a cone-specific regeneration pathway is supported by biochemical and genetic data. Earlier work implicated Müller glia cells of the inner retina in the recycling of the visual chromophore (Goldstein and Wolf, 1973; Hood and Hock, 1973; Saari et al., 1982; Bunt-Milam and Saari, 1983; Saari and Bredberg, 1987).

Work on the dynamics of retinoid accumulation in the cone-dominant chicken retina found evidence for two pools of 11-*cis*-retinyl esters with different depletion dynamics (Trevino et al., 2005). Genetic evidence for an alternative pathway was provided by knock-down studies of the retinoid isomerase Rpe65, a pivotal component of the canonical visual cycle. Depletion of Rpe65 in the cone-dominant zebrafish retina leads to decreased 11-*cis*-retinal levels but does not exert any effect on the larval optokinetic response, which originates exclusively in cone photoreceptors at this developmental stage (Schonthaler et al., 2007)

Mata et al. (2005) identified several novel enzymatic activities in the chicken retina that constitute likely components of an alternative cone-specific visual cycle. Consistent with earlier work, these components are suggested to be located in cone pho-
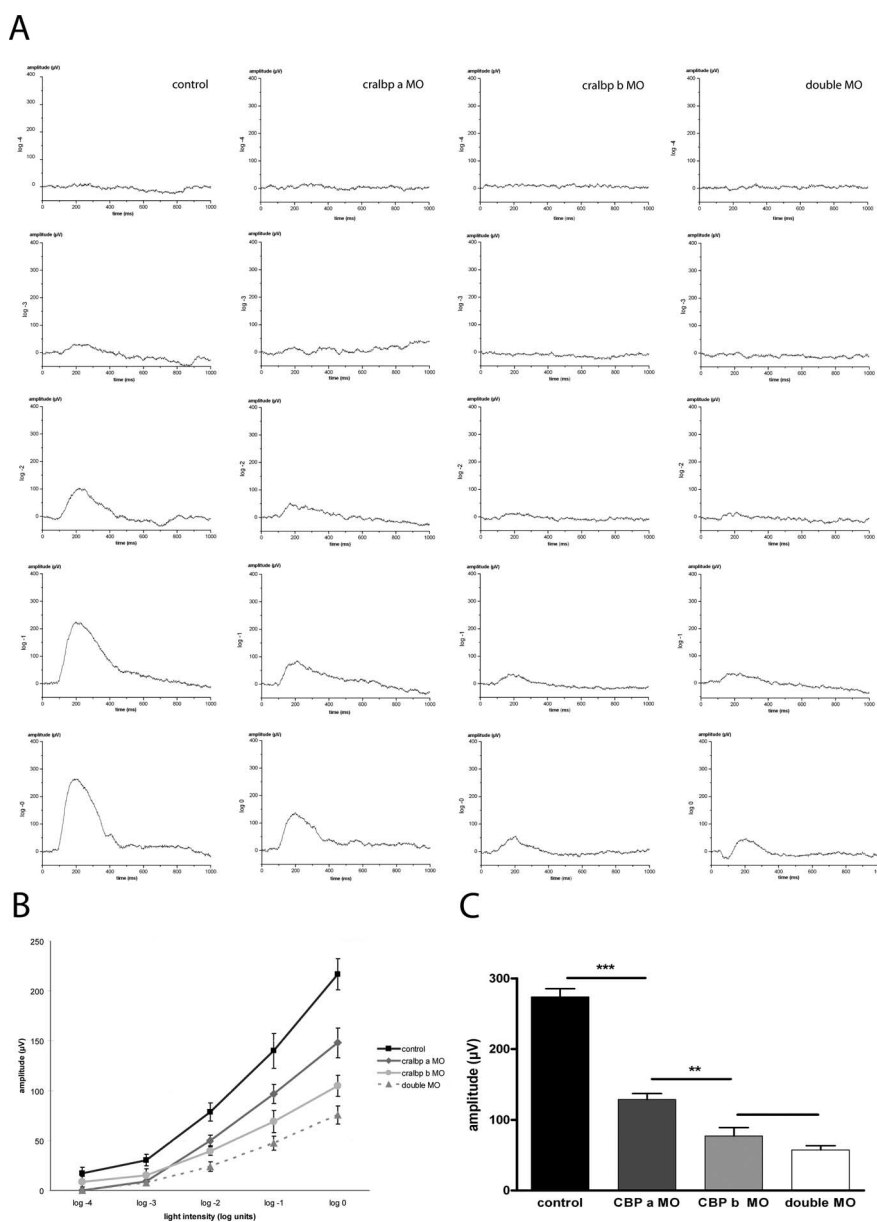

Figure 6. ERG recordings of *cralbp a, b,* and double-morpholino-injected larvae. **A,** Typical ERG traces of dark-adapted 5 dpf control and morpholino-injected larvae (*cralbp a,* 1 mm; *cralbp b,* 700 μm; coinjected at 800 μm/500 μm) at different light intensities (log 0 corresponds to 6300 lux or 6.9 mW/cm²). **B,** Graph depicting the intensity–response function of controls compared with morpholino-injected larvae (data points represent means of $n = 10$ larvae for each light intensity ± SEM). **C,** Table of averaged saturated b-wave responses (means of $n = 12$ larvae ± SD) of controls compared with morpholino-injected larvae (light intensity, 6000 lux). Statistical analysis was performed with GraphPad Prism software using one-way ANOVA on measured data ($p < 0.001$ for *cralbp a* and *b* and double MO compared with wild type; $p < 0.01$ for *cralbp a* compared with *cralbp b* MO).

toreceptors and Müller glia cells. None of these components has been identified yet.

To initiate a molecular characterization of these components, we used the cone-dominant zebrafish retina. We reasoned that retinoid-binding proteins might be common components to both the canonical and the alternative visual cycle.

Retinoid-binding proteins (CRBP, IRBP, CRALBP) have been shown to have a variety of different functions in the canonical visual cycle (Bridges et al., 1984; Okajima et al., 1990; Pepperberg et al., 1993; Palczewski et al., 1999). CRALBP protein specifically binds 11-*cis*-retinoids (Bunt-Milam and Saari, 1983; Saari and Bredberg, 1987) and has an important role in the isomerization
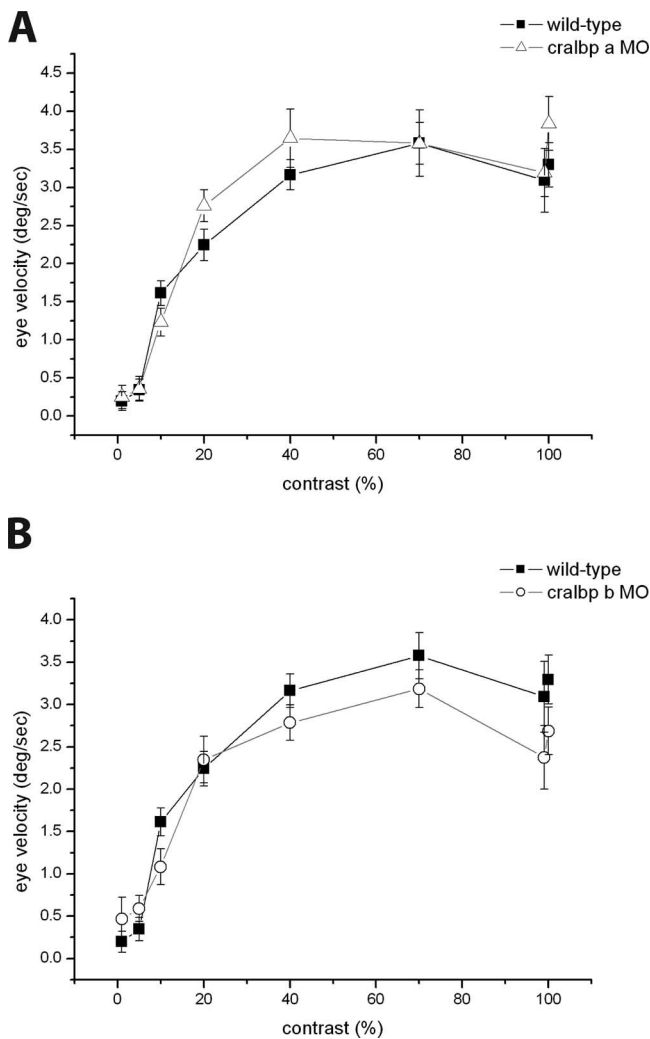
Figure 7. OKR recordings of *cralbp a* and *b* morpholino-injected larvae compared with wild type. OKR responses of 5 dpf controls compared with *cralbp* morpholino-injected larvae triggered by gratings of varying contrast (0 –99%). Measurements were done under dark-adapted conditions with averaged responses of $n = 12$. Statistical analysis was performed using a bootstrap resampling test of pooled data; the significance level was chosen to be 5% for all recordings ($p < 0.05$ for *cralbp b* MO at contrasts between 70 and 100%). **A**, Wild-type versus *cralbp a* morpholino-injected larvae. **B**, Wild-type versus *cralbp b* morpholino-injected larvae ($p < 0.05$ for contrasts >40%).

and oxidation steps of the visual cycle (Saari and Bredberg, 1987; Saari et al., 2001; Golovleva et al., 2003).

Here, we report the identification of two paralogous *cralbp* genes in the zebrafish genome. The family of ray-finned (teleost) fish has undergone an additional whole-genome duplication in the course of its evolution, as compared with the other vertebrate groups (Taylor et al., 2003; Meyer and Van de Peer, 2005). As a consequence, a sizable number of genes are found in duplicate versions. The stable occurrence of such paralogs is likely caused by either neofunctionalization or subfunctionalization, because the retention of functional redundancy over the course of many millions of years is unlikely.

We found complementary expression patterns for the two zebrafish *cralbp* paralogs, lending strong support for a subfunctionalization event in which the function of one ortholog in two cell types is split between the paralogs. Indeed, we found one paralog expressed in Müller glia cells and the other in the RPE,

enabling us to separately probe the function of this protein and its involvement in the two pathways.

We selectively depleted the proteins separately by morpholino-mediated translation blockage. Functional analysis using behavioral and electrophysiological assays of larval zebrafish devoid of either protein (Cralbp a or b), or both, revealed that a knock-down resulted in impaired vision. We have observed that loss of Cralbp b protein, which is localized in Müller glia cells, leads to more pronounced effects on photoreceptor function, as measured by ERG and OKR recordings. However, downregulation of the RPE-specific Cralbp a variant also causes a decrease in b-wave amplitude. Biochemical analysis confirmed that loss of Cralbp protein leads to reduced levels of 11-*cis*-retinal in photoreceptors after photobleaching.

Thereby we showed that Cralbp not only is a component of the canonical visual cycle but also functions in the cone-specific alternative visual cycle. In the canonical visual cycle, Cralbp acts downstream of Rpe65 in visual chromophore regeneration (Saari and Bredberg, 1987; Saari et al., 2001; Golovleva et al., 2003). A knock-down of Cralbp a or Rpe65 leads to a significant decrease in 11-*cis*-retinal regeneration after bleaching (Fig. 5) (Schonthaler et al., 2007). Interestingly, both Cralbp a- and Rpe65-deficient larvae showed no deficits in optokinetic response tests (Fig. 7) (Schonthaler et al., 2007). This finding is likely explained by the existence of an alternative visual cycle that relies on Cralbp b expression in Müller cells. Cralbp b-deficient larvae showed both a reduction of 11-*cis*-retinal levels and deficits in visual behavior tests. As in the canonical visual cycle, Cralbp might act downstream of a Müller cell-specific retinoid isomerase on 11-*cis*-retinal regeneration (Mata et al., 2005). Because cone vision was not completely abolished in either Cralbp a- and Cralbp b-deficient larvae, our data argue for an involvement of both visual cycles in cone pigment regeneration. This characteristic might be explained by the fact that in Cralbp b deficiency, cones might be supplied by 11-*cis*-retinal produced by the canonical visual cycle. Conversely, in Cralbp a-depleted larvae, cones may consume 11-*cis*-retinal produced by the Müller cell-specific visual cycle. In this context, it is noteworthy that a lack of Cralbp does not completely abolish 11-*cis*-retinal regeneration, as evidenced by the analysis of $Cralbp^{-/-}$ mice. This characteristic might also explain the persisting 11-*cis*-retinal in the larvae depleted for both Cralbp paralogs. In future studies, the relative importance of the canonical and alternative visual cycle for cone visual pigment regeneration needs to be established. It likely depends on the species-specific photoreceptor composition and arrangement of the outer retina. We expect that the reliance of cone pigment regeneration on the non-canonical pathway will increase with the increase in rod contribution to zebrafish vision occurring at later larval stages (Branchek, 1984). Our data are in full agreement with a recent study conducted in patients suffering from Leber congenital amaurosis. Such patients carry a mutated version of the retinoid isomerase RPE65 and, as a consequence, they exhibit cone photoreceptor loss even at the earliest stages of disease. Strikingly, this loss is not complete, and residual cone structure and function persist for decades (Jacobson et al., 2007). We conclude that the RPE65-based visual cycle must be important for cone function, but there must also exist an alternative pathway for visual pigment regeneration, which could explain cone survival.

In summary, we have identified the first molecular component of the cone-specific alternative visual cycle, using the favorable genetics of the cone-dominant zebrafish. The two paralogs of the retinoid-binding protein Cralbp play a role in two separate

visual pigment regeneration pathways, as evidenced by biochemical, genetic, physiological, and behavioral data. These visual cycles are located in two separate compartments in the zebrafish retina: the canonical visual cycle in the RPE and the proposed cone-specific cycle in Müller glia cells. Because interfering with both pathways leads to functional deficits in the cone-dominant retina of the zebrafish, we propose that cone photoreceptors use both mechanisms of pigment regeneration. Both visual cycles depend on the function of the retinoid-binding protein Cralbp.

References

Branchek T (1984) The development of photoreceptors in the zebrafish, brachydanio rerio. II. Function. J Comp Neurol 224:116–122.

Bridges CD, Alvarez RA, Fong SL, Gonzalez-Fernandez F, Lam DM, Liou GI (1984) Visual cycle in the mammalian eye. Retinoid-binding proteins and the distribution of 11-cis retinoids. Vision Res 24:1581–1594.

Bunt-Milam AH, Saari JC (1983) Immunocytochemical localization of two retinoid-binding proteins in vertebrate retina. J Cell Biol 97:703–712.

Dahm R, Geisler, R, Nüsslein-Volhard C (2005) Zebrafish (*Danio rerio*) genome and genetics. Weinheim, Germany: Wiley-VCH.

Goldstein EB, Wolf BM (1973) Regeneration of the green-rod pigment in the isolated frog retina. Vision Res 13:527–534.

Golovleva I, Bhattacharya S, Wu Z, Shaw N, Yang Y, Andrabi K, West KA, Burstedt MS, Forsman K, Holmgren G, Sandgren O, Noy N, Qin J, Crabb JW (2003) Disease-causing mutations in the cellular retinaldehyde binding protein tighten and abolish ligand interactions. J Biol Chem 278:12397–12402.

Hood DC, Hock PA (1973) Recovery of cone receptor activity in the frog's isolated retina. Vision Res 13:1943–1951.

Jacobson SG, Aleman TS, Cideciyan AV, Heon E, Golczak M, Beltran WA, Sumaroka A, Schwartz SB, Roman AJ, Windsor EA, Wilson JM, Aguirre GD, Stone EM, Palczewski K (2007) Human cone photoreceptor dependence on RPE65 isomerase. Proc Natl Acad Sci U S A 104:15123–15128.

Jin M, Li S, Moghrabi WN, Sun H, Travis GH (2005) Rpe65 is the retinoid isomerase in bovine retinal pigment epithelium. Cell 122:449–459.

Makhankov YV, Rinner O, Neuhauss SC (2004) An inexpensive device for non-invasive electroretinography in small aquatic vertebrates. J Neurosci Methods 135:205–210.

Mata NL, Radu RA, Clemmons RC, Travis GH (2002) Isomerization and oxidation of vitamin a in cone-dominant retinas: a novel pathway for visual-pigment regeneration in daylight. Neuron 36:69–80.

Mata NL, Ruiz A, Radu RA, Bui TV, Travis GH (2005) Chicken retinas contain a retinoid isomerase activity that catalyzes the direct conversion of all-trans-retinol to 11-cis-retinol. Biochemistry 44:11715–11721.

McBee JK, Van Hooser JP, Jang GF, Palczewski K (2001) Isomerization of 11-cis-retinoids to all-trans-retinoids in vitro and in vivo. J Biol Chem 276:48483–48493.

Meyer A, Van de Peer Y (2005) From 2R to 3R: evidence for a fish-specific genome duplication (FSGD). Bioessays 27:937–945.

Moiseyev G, Chen Y, Takahashi Y, Wu BX, Ma JX (2005) RPE65 is the isomerohydrolase in the retinoid visual cycle. Proc Natl Acad Sci U S A 102:12413–12418.

Muniz A, Villazana-Espinoza ET, Hatch AL, Trevino SG, Allen DM, Tsin AT (2007) A novel cone visual cycle in the cone-dominated retina. Exp Eye Res 85:175–184.

Nasevicius A, Ekker SC (2000) Effective targeted gene 'knockdown' in zebrafish. Nat Genet 26:216–220.

Okajima TI, Pepperberg DR, Ripps H, Wiggert B, Chader GJ (1990) Interphotoreceptor retinoid-binding protein promotes rhodopsin regeneration in toad photoreceptors. Proc Natl Acad Sci U S A 87:6907–6911.

Palczewski K, Van Hooser JP, Garwin GG, Chen J, Liou GI, Saari JC (1999) Kinetics of visual pigment regeneration in excised mouse eyes and in mice with a targeted disruption of the gene encoding interphotoreceptor retinoid-binding protein or arrestin. Biochemistry 38:12012–12019.

Palczewski K, Hofmann KP, Baehr W (2006) Rhodopsin—advances and perspectives. Vision Res 46:4425–4426.

Pepperberg DR, Okajima TL, Wiggert B, Ripps H, Crouch RK, Chader GJ (1993) Interphotoreceptor retinoid-binding protein (IRBP). Molecular biology and physiological role in the visual cycle of rhodopsin. Mol Neurobiol 7:61–85.

Redmond TM, Poliakov E, Yu S, Tsai JY, Lu Z, Gentleman S (2005) Mutation of key residues of RPE65 abolishes its enzymatic role as isomerohydrolase in the visual cycle. Proc Natl Acad Sci U S A 102:13658–13663.

Rinner O, Rick JM, Neuhauss SC (2005a) Contrast sensitivity, spatial and temporal tuning of the larval zebrafish optokinetic response. Invest Ophthalmol Vis Sci 46:137–142.

Rinner O, Makhankov YV, Biehlmaier O, Neuhauss SC (2005b) Knockdown of cone-specific kinase GRK7 in larval zebrafish leads to impaired cone response recovery and delayed dark adaptation. Neuron 47:231–242.

Saari JC, Bredberg DL (1987) Photochemistry and stereoselectivity of cellular retinaldehyde-binding protein from bovine retina. J Biol Chem 262:7618–7622.

Saari JC, Bredberg L, Garwin GG (1982) Identification of the endogenous retinoids associated with three cellular retinoid-binding proteins from bovine retina and retinal pigment epithelium. J Biol Chem 257:13329–13333.

Saari JC, Nawrot M, Kennedy BN, Garwin GG, Hurley JB, Huang J, Possin DE, Crabb JW (2001) Visual cycle impairment in cellular retinaldehyde binding protein (CRALBP) knockout mice results in delayed dark adaptation. Neuron 29:739–748.

Schoenlein RW, Peteanu LA, Mathies RA, Shank CV (1991) The first step in vision: femtosecond isomerization of rhodopsin. Science 254:412–415.

Schonthaler HB, Lampert JM, Isken A, Rinner O, Mader A, Gesemann M, Oberhauser V, Golczak M, Biehlmaier O, Palczewski K, Neuhauss SC, von Lintig J (2007) Evidence for RPE65-independent vision in the cone-dominated zebrafish retina. Eur J Neurosci 26:1940–1949.

Stecher H, Gelb MH, Saari JC, Palczewski K (1999) Preferential release of 11-cis-retinol from retinal pigment epithelial cells in the presence of cellular retinaldehyde-binding protein. J Biol Chem 274:8577–8585.

Stryer L (1986) Cyclic GMP cascade of vision. Annu Rev Neurosci 9:87–119.

Taylor JS, Braasch I, Frickey T, Meyer A, Van de Peer Y (2003) Genome duplication, a trait shared by 22000 species of ray-finned fish. Genome Res 13:382–390.

Trevino SG, Villazana-Espinoza ET, Muniz A, Tsin AT (2005) Retinoid cycles in the cone-dominated chicken retina. J Exp Biol 208:4151–4157.

von Lintig J, Vogt K (2000) Filling the gap in vitamin A research. Molecular identification of an enzyme cleaving beta-carotene to retinal. J Biol Chem 275:11915–11920.

Wald G (1968) The molecular basis of visual excitation. Nature 219:800–807.

Westerfield M (1994) The zebrafish book: a guide for the laboratory use of zebrafish (*Danio rerio*). Eugene, OR: University of Oregon.

Winston A, Rando RR (1998) Regulation of isomerohydrolase activity in the visual cycle. Biochemistry 37:2044–2050.